15th Australasian Fluid Mechanics Conference
The University of Sydney, Sydney, Australia
13-17 December 2004

# Effect of Initial Conditions on the Far Field of a Round Jet

**P. Burattini, R. A. Antonia and S. Rajagopalan**

Discipline of Mechanical Engineering
University of Newcastle, NSW, 2308 AUSTRALIA

## Abstract

The effect of initial conditions on the far field of a turbulent round jet ($R_\lambda \simeq 450$) has been examined using hot-wire measurements. Two types of initial conditions have been examined: the unperturbed jet, issuing from a nozzle in a laminar state, and the perturbed jet, where a woven grid is placed at the jet outlet in order to interfere with the initial development of the jet. Turbulent integral quantities and small scale characteristics show that the flow is partly reminiscent of the initial stages of the jet development, as modified by the grid. While the first- and second-order velocity statistics are affected only in terms of the virtual origin, length scales (such as the Kolmogorov and the Taylor scale) show also a different decay rate, under modified initial conditions. The similarity of the second-order structure functions is unaltered by the grid.

## Introduction and Background

The concept of similarity has played a central role in fluid dynamics research. Blasius applied this approach to the study of the laminar boundary layer over a flat plate, showing that there is compatibility between the equations of motion and a universal velocity profile. From this, the actual profile at any streamwise station can be derived. The Blasius approach for *laminar flow* paved the way for its extension to the similarity analysis of *turbulent flows* (e.g., plane and axisymmetric jets and wakes, [16, 20, 21, 22, 24]).

Similarity of multi-scale statistics (as opposed to one-point statistics), such as spectra or structure functions of turbulent quantities, has been the subject of more recent attention. An attempt to investigate the similarity of multi-point statistics of homogeneous isotropic turbulence, starting from the spectral dynamical equation, has been made by George [10]. He showed that self-similarity of the velocity spectra, normalized by the Taylor scale and mean kinetic energy, is compatible with this equation. More recently, a similar conclusion was obtained for velocity structure functions by Antonia et al. [2].

However, the validity of universal similarity in turbulent flows has been criticised from time to time. George [9, 10] noted that there is no *a priori* reason why the influence of initial conditions should be ruled out from the outset. If true, this argument would preclude *universal* (namely, unchanged from one realization of the same flow to another) similarity solutions. Even though George's suggestion remains qualitative in nature, since there is no formal way of taking explicitly into account the initial conditions, it seems plausible, considering the large scatter in experimental data in nominally identical flows.

Besides the role of initial conditions, but perhaps not separately from these, is the effect coherent structures may have on the achievement of similarity. The evolution of the large scales could preclude a state of similarity for the complete spectrum, because the energy may be concentrated in a few modes with strong interactions between them. The available evidence seems convincing. For instance, it has been noticed that in far field of a 2D wake behind a bluff body the flow properties depend on the coherent structures and how they were created in relation to the geometrical details of the wake generator (solidity, shape) [25, 3]. Arguably, the role of coherent structures can be assessed in a more specific manner compared to that of the initial conditions. Direct measurements, say of coherent vorticity or spatial correlation, can show the influence of the large scale structures.

In the round jet, evidence of the relationship between initial conditions, coherent structures, and similarity is not yet complete. If we discard comparisons between different experimental set-ups (since the results may be biased by different arrangements and experimental techniques) there is not much left in the literature from which a sound conclusion can be drawn on this issue. Although many studies have been indeed devoted to the modification of initial conditions and their effect on velocity and scalar in the developing region of the flow ([11, 17, 23, 28]), the extension of the analysis to the far field has not previously been considered. When the developed region is explored, the initial conditions are, usually, only briefly discussed. For instance in two of the most recent investigations on the far field of a round jet [12, 19] the initial conditions are not described in great detail.

In previous works [5, 8] we examined the effect of different initial conditions on the developing region of a round jet (within 12 diameters from the exit). The disturbances created by a grid at the exit inhibited the shear layer mode and delayed the preferred mode. The extension of the potential core was increased by nearly 50% in the disturbed case. The effects of disc and annular-shaped grids have been also investigated in connection to the near field of a round jet, [14]. Here we want to document the possible influences of the initial conditions on the far field of a jet. This problem has been discussed in two recent papers [26, 27], where two jets (one issuing from a contraction nozzle and the other from a pipe) were compared. The authors concluded that there was no appreciable effect on the turbulent energy distribution, due to the different initial conditions, at 20 diameters downstream from the exit.

A check of the effect of the initial and boundary conditions is apparently more within the reach of direct numerical simulation. The work of Boersma et al. [4] (see also [15]) has tried to address this issue by investigating the effect of two different initial conditions: a top-hat exit velocity profile and another with the streamwise velocity overshooting in proximity of the boundary layer. The authors claimed that: "evidence is presented in support of the suggestion by George [9] that the details of self-similarity depend on the initial conditions". However, these authors ran simulations only up to 45 diameters, where the flow is only starting to be similar [22]. In a recent work [7] the similarity properties of the velocity spectra and structure functions have been studied experimentally in a turbulent round jet. It was shown that the collapse of these quantities was best when the Taylor microscale and the mean turbulent kinetic energy were adopted as similarity scales.

## Experimental Details

The jet was generated using an open circuit wind tunnel, located in a relatively large laboratory. The tunnel contains a variable speed centrifugal blower, a diffuser, a settling chamber, and a contraction with an area ratio of 85:1. Screens and a honeycomb are fitted inside the settling chamber to reduce the turbulence level and to straighten the flow. The outlet circular nozzle has a diameter $D = 55$ mm. The velocity probe could be traversed along the streamwise ($x$), lateral ($y$), and vertical ($z$) directions with a resolution of 0.1 mm, 0.1 mm and 0.01 mm respectively. Two velocity components were measured: $u$, in the streamwise direction, and $v$ in the lateral (or radial) direction. The corresponding uppercase quantities refer to the time-averaged values and a prime denotes the rms value.

Two types of exit conditions are investigated: the unperturbed jet (or case $A$), as it exits from a smooth contraction, and the perturbed jet (case $B$). The modification of the initial conditions was achieved by placing a grid at the jet outlet. Details of the grid, composed of rigid woven round steel wires, are given in table 1. The reference exit velocity, $U_j$, was fixed at $\simeq 35$ ms$^{-1}$ and 32.5 ms$^{-1}$ for case A and B, respectively. This yielded an exit Reynolds number, $Re_D = DU_j/\nu$ ($\nu$ is the kinematic viscosity of the air), of $1.3 \times 10^5$ and $1.2 \times 10^5$, for the two cases. Further details on the initial conditions of the perturbed and unperturbed cases can be found in [5]. Measurements were carried out in the far field of the jets for $30 \leqslant x/D \leqslant 90$ (see also [7] for a detailed description of the flow field characteristics).

The velocity was acquired by means of in-house hot wires and DISA anemometers (55M01 model). X-wire probes, with an angle between the wires of nearly $90^\circ$ and a lateral separation between the wires of approximately 0.8 mm, were operated at an overheat of 1.5. The hot wires were etched from Pt-10% Rh to a diameter of $d_w = 2.5\mu$m and the active length $l_w$ was chosen so as to have an aspect ratio $l_w/d_w$ of nearly 200.

Velocity and angle calibrations were carried out *in situ* at the jet exit plane. The X-wire was calibrated at several values of speed and angle in the ranges of $40^\circ$ (in steps of $10^\circ$) and $0.9 - 17.2$ ms$^{-1}$, respectively. This set of values was used as a look-up-table (LUT), during the data reduction step, to estimate the velocity through spline interpolations. The LUT method was verified to give, for mean longitudinal velocities below 6 ms$^{-1}$, more reliable results than the common effective angle method [6], which assumes a constant coefficient of sensitivity for the lateral velocity. Single wire data were used as a check of the X-wire response, and differences in the mean values of the streamwise velocity were always below 2%. The anemometer signals were acquired by means of a 16-bit AD board. Uncertainties in the mean and rms fluctuation velocities were about 0.8% and 4%, respectively, as calculated by repeating the measurements 30 times at $60D$ and applying standard error estimations (1:20 odds) [18].

### Velocity and Length Scales

The decay of the mean longitudinal velocity, $U_0$, along the axis is shown in figure 1. Data were least squares fitted according to the model equation $\alpha = C_\alpha^{-1}(x - x_{0_\alpha})/D$, where $\alpha$ refers to a generic quantity (a length or a velocity scale), $C_\alpha$ represents the decay rate (or growth rate, for the length scales) coefficient and $x_{0_\alpha}$ is the virtual origin. From this figure, it is clear that the decay rate (measured by the slope of the least squares fit to the data) is unchanged between the two jets (see also table 2). There is, however, a downstream shift in the decay origin for case $B$. This can be appreciated better from the inset in figure 1, which focuses on the initial region of the jet, from [5]. In this reference it was shown that the grid delayed by nearly two diameters the start of the decay in the axial direction. The axial decay of $u'$ (figure 2) is inversely linear, as expected, with an almost identical decay rate for both cases, but different virtual origins. Again, the inset in the figure shows that the initial stage of the jet is responsible for the shift.

It is worth comparing the mean turbulent energy decay of the jets with that of grid turbulence. In the latter case, $u'^2$ decays following a power law with decay rates varying according to the initial conditions, a typical range being $-1.1 < m < -1.3$ [20] ($m$ is the coefficient of the power law). Parameters such as grid solidity, geometry (planar, biplanar, woven) and shape of the grid elements have a discernible influence on the decay rate of the mean energy in the equilibrium region ($x/M \geqslant 40$, $M$ is the mesh size) [13]. At variance with grid turbulence, the decay rate of $u'^2$ for the jet is unaltered by the initial conditions, the effect being restricted to a shift in the origin.

The ratio of the turbulence intensities in the streamwise and radial directions, $u'/v'$, is provided in figure 3. The two jets attain almost exactly the same constant value ($\simeq 1.25$) along the axis, showing that, in the range investigated, an equilibrium between the two components is reached in both cases. The ratio of the integral scales (which are defined by the first zero-crossing of the autocorrelation function of the velocity fluctuation), $L_u/L_v$, is about 1.75 (same figure), but it shows a comparatively larger scatter. This can be partly related to the definition of the integral scale, which is somewhat ill-conditioned. Note that the isotropic value of this ratio is 2, thus significantly higher than in the present cases. The ratio $u'/v' (\simeq 1.2)$, although typical for a round jet [12], is also far from the isotropic value (=1). In figure 3, we also report the turbulence intensity, $u'/U_0$: its value is around 25%, as expected for an unconfined jet [12, 19].

The rate of growth of the Kolmogorov length scale ($\eta \equiv \left(\nu^3/\langle\varepsilon\rangle\right)^{1/4}$, where $\langle\varepsilon\rangle$ is the mean energy dissipation rate and angular brackets denote time averaging) and the Taylor microscale ($\lambda \equiv u'/(\partial u/\partial x)'$) is given in figure 4. Compared to the velocity scales, the behaviour of $\eta$ and $\lambda$ is more sensitive to the initial conditions. Case $B$ has a faster decay rate for these two quantities, while the virtual origin is located further downstream (table 3), compared to case $A$. This is in the same direction as the shift for $U_j/U_0$ and $U_j/u'$. The circular jet is one of the (few) flows for which the turbulent Reynolds number, $R_\lambda = \lambda u'/\nu$, is considered to be constant along the streamwise direction [22]. However, it is clear that this is true only if the virtual origins of $\lambda$ and $u'$ are the same, zero being a special case. From the present results, it seems that this is not generally valid. However, it can be noted that, as $x/D$ becomes larger, the product of $\lambda$ and $u'$ becomes less sensitive to the value of the virtual origins. Thus $R_\lambda$ approaches a constant value.

| Case | $U_j$ (ms$^{-1}$) | $M$ (mm) | $t$ (mm) | $D/M$ – | $\sigma$ – |
|---|---|---|---|---|---|
| $A$ (unperturbed) | 35.0 | – | – | – | – |
| $B$ (perturbed) | 32.5 | 3.2 | 0.7 | $\simeq 16$ | 0.44 |

Table 1: Jet configurations investigated. $M$: mesh size; $t$: mesh wire diameter; $\sigma$: solidity.

| Case | $C_{U_j/U_0}$ | $x_{0_{U_j/U_0}}/D$ | $C_{U_j/u'}$ | $x_{0_{U_j/u'}}/D$ |
|---|---|---|---|---|
| $A$ | 5.98 | 4.32 | 1.51 | $-1.43$ |
| $B$ | 6.06 | 5.68 | 1.50 | 1.01 |

Table 2: Decay rate characteristics of the velocity scales.

### Similarity of the Structure Functions

The second-order structure functions of the turbulent kinetic energy, $\left\langle(\delta q)^2\right\rangle = \left\langle(\delta u)^2\right\rangle + 2\left\langle(\delta v)^2\right\rangle$, where $\delta\bullet \equiv \bullet(x+r) -$

| Case | $C_\eta$ $(\mathrm{m}^{-1})$ | $x_{0_\eta}/D$ – | $C_\lambda$ $(\mathrm{m}^{-1})$ | $x_{0_\lambda}/D$ – |
|---|---|---|---|---|
| $A$ | $3.38\times10^5$ | $-1.79$ | $8.08\times10^3$ | $-3.03$ |
| $B$ | $3.08\times10^5$ | $1.96$ | $7.64\times10^3$ | $-0.08$ |

Table 3: Decay rate characteristics of the length scales.

$\bullet(x)$ is the difference of a quantity $\bullet(=u$ or $v)$ between two points separated by $r$ along the streamwise direction are given in figure 5. Since $R_\lambda$ is constant along the axis (with the specifications given before), in each case these functions are in similarity [7]. This is reflected in the collapse of the normalized profiles of $\left\langle(\delta q)^2\right\rangle$ measured at different axial locations. However, the initial conditions do not alter the collapse; this would have been apparent had the structure functions not been shifted to improve clarity. The third-order structure function $\left\langle(\delta u)(\delta q)^2\right\rangle$ (not shown here) indicate that the similarity is also valid at this order, even though the scatter is larger, as expected for odd-order moments. It is worth noting that the similarity condition of the structure functions involves both velocity and length scales, since they are both used to normalize the profiles. Thus, even though the length scales are more sensitive to the initial conditions, the normalized form of $\left\langle(\delta q)^2\right\rangle$ can absorb these variations to yield a unique self-similar profile.

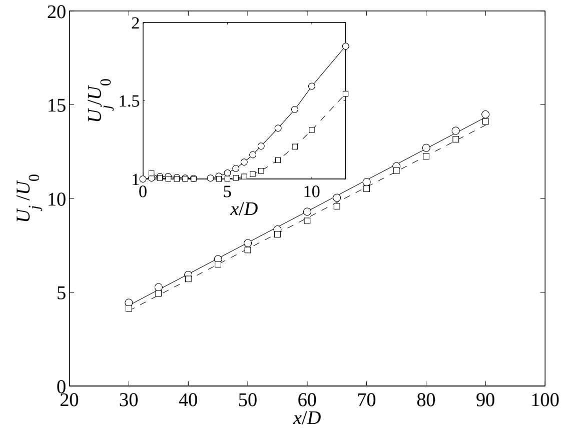


Figure 1: Mean longitudinal velocity along the axis: $-\circ$, case $A$; - -$\square$, case $B$. Inset: developing region (from [5]).

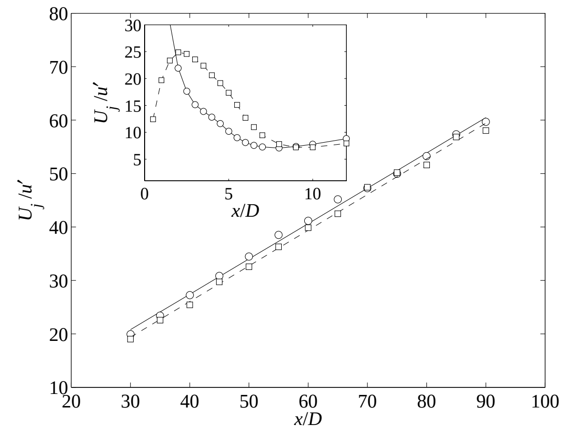


Figure 2: Rms longitudinal velocity along the axis: $-\circ$, case $A$; - -$\square$, case $B$. Inset: developing region (from [5]).

#### Conclusions

Similarity ideas continue to play a central role in the description of fluids dynamics. Recently, it has become evident that universal similarity solution are not possible for certain types of flows [1, 2, 9, 10]. For instance, grid turbulence, arguably the most basic type of turbulent flow that can be set up in a laboratory, shows a dependence on the initial generation of the flow [13]. In this regard, it can be speculated that the details of the large scales production behind the grid can have a lasting influence on the subsequent evolution of the flow [9] in terms of the redistribution of energy among the velocity components and the mean energy decay rate. The present results, for the far field of a perturbed and an unperturbed round jet, show that, on one hand, basic quantities, such as the decay rate of the mean velocity and mean energy, are not influenced by a modification in the initial conditions in a significant way; for these two quantities, only a shift in the virtual origin is detected. On the other hand, the decay of the Kolmogorov and Taylor length scales is modified in terms of the growth rate and virtual origin, even though the former remains linear. Profiles of the normalized second-order velocity structure functions indicate that similarity is not affected by the initial conditions. This is at odds with grid turbulence, where the initial conditions have an influence on the shape of the second-order structure functions even at large distance from the grid. It is plausible that, in the case of the jet, the coherent structures generated in the developing region evolve more rapidly towards an equilibrium state, compared to grid turbulence. This is compatible with the observed self-similarity of the multi-scale distribution of the turbulent energy measured at different axial locations.

#### Acknowledgments

The support of the Australian Research Council is gratefully acknowledged.

#### References


[1] Antonia, R. A. and Burattini, P., Small-scale turbulence: How universal is it?, in *15th Australasian Fluid Mechanics Conference*, University of Sydney, 2004.

[2] Antonia, R. A., Smalley, R. J., Zhou, T., Anselmet, F. and Danaila, L., Similarity of energy structure functions in decaying homogeneous isotropic turbulence, *J. Fluid Mech.*, **487**, 2003, 245–269.

[3] Antonia, R. A., Zhou, T. and Romano, G. P., Small-scale turbulence characteristics of two-dimensional bluff body wakes, *J. Fluid Mech.*, **459**, 2002, 67–92.

[4] Boersma, B. J., Brethouwer, G. and Nieuwstadt, F. T. M., A numerical investigation on the effect of the inflow conditions on the self-similar region of a round jet, *Phys. Fluids*, **10**, 1998, 899–909.

[5] Burattini, P., Antonia, R., Rajagopalan, S. and Stephens, M., Effect of initial conditions on the near-field development of a round jet, *Exp. Fluids*, **37**, 2004, 56–64.

[6] Burattini, P. and Antonia, R. A., The effect of different X-wire calibration schemes on some turbulence statistics, *Accepted for publication in Exp. Fluids, 2005*.

[7] Burattini, P., Antonia, R. A. and Danaila, L., Similarity in the far field of a turbulent round jet, *Accepted for publication in Phys. Fluids, 2005*.

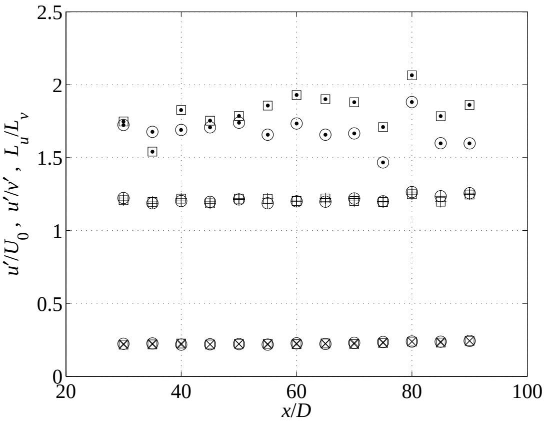


Figure 3: Axial variations of $u'/v'$, $u'/U_0$ and $L_u/L_v$. $+$, $u'/v'$; $\times$, $u'/U_0$; $\bullet$, $L_u/L_v$. $\circ$, case *A*; $\square$, case *B*.

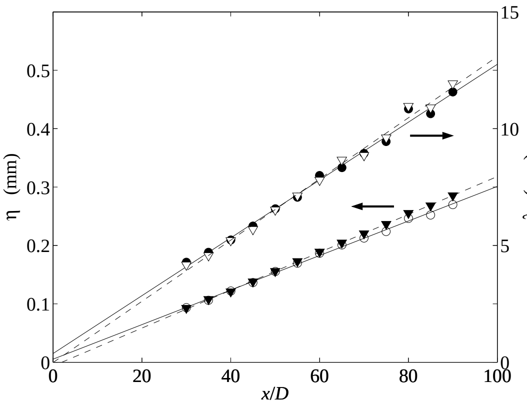


Figure 4: Axial growth of the Kolmogorov and Taylor microscales. $-\circ$, $\eta$ case *A*; - -$\blacktriangledown$, $\eta$ case *B*; $-\bullet$, $\lambda$ case *A*; - -$\triangledown$, $\lambda$ case *B*.

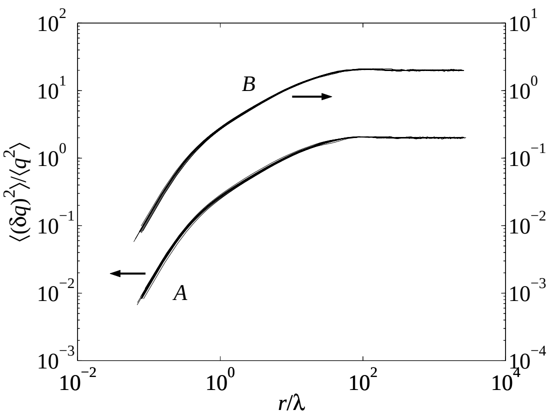


Figure 5: Second-order structure functions of the turbulent kinetic energy along the axis of the jet ($30 \leqslant x/D \leqslant 90$) for cases *A* and *B*.


[8] Burattini, P. and Djenidi, L., Velocity and passive scalar characteristics in a round jet with grids at the nozzle exit, *Flow Turbul. Combust.*, **72**, 2004, 199–218.

[9] George, W. K., The self-preservation of turbulent flows and its relation to initial conditions and coherent structures, in *Advances in turbulence*, editors W. K. George and R. Arndt, Springer, Berlin, 1989, 39–74.

[10] George, W. K., The decay of homogeneous isotropic turbulence, *Phys. Fluids A*, **4**, 1992, 1492–1509.

[11] Husain, Z. D. and Hussain, A. K. M. F., Natural instability of free shear layers, *AIAA J.*, **21**, 1983, 1512–1517.

[12] Hussein, H. J., Capp, S. P. and George, W. K., Velocity measurements in a high-Reynolds-number, momentum-conserving, axisymmetric, turbulent jet, *J. Fluid Mech.*, **258**, 1994, 31–75.

[13] Lavoie, P., Antonia, R. A. and Djenidi, L., Effect of grid geometry on the scale-by-scale budget of decaying turbulence, in *15th Australasian Fluid Mechanics Conference*, University of Sydney, 2004.

[14] Lehman, R., Rajagopalan, S., Burattini, P. and Antonia, R. A., Axisymmetric jet control using passive grids, in *15th Australasian Fluid Mechanics Conference*, University of Sydney, 2004.

[15] Lubbers, C. L., Brethouwer, G. and Boersma, B. J., Simulation of the mixing of a passive scalar in a round turbulent jet, *Fluid Dyn. Res.*, **28**, 2001, 189–208.

[16] Mathieu, J. and Scott, J., *An Introduction to Turbulent Flow*, Cambridge University Press, Cambridge, 2000.

[17] Mi, J., Nobes, D. S. and Nathan, G. J., Influence of jet exit conditions on the passive scalar field of an axisymmetric free jet, *J. Fluid Mech.*, **432**, 2001, 91–125.

[18] Moffat, R. J., Describing the uncertainties in experimental results, *Exp. Therm. Fluid Sci.*, **1**, 1988, 3–17.

[19] Panchapakesan, N. R. and Lumley, J. L., Turbulence measurements in axisymmetric jets of air and helium. Part 1. Air jet, *J. Fluid Mech.*, **246**, 1993, 197–223.

[20] Pope, S. B., *Turbulent Flows*, Cambridge University Press, Cambridge, 2000.

[21] Schlichting, H., *Boundary-layer Theory*, McGraw–Hill, New York, 1979.

[22] Tennekes, H. and Lumley, J. L., *A First Course in Turbulence*, MIT Press, Cambridge, MA, 1972.

[23] Tong, C. and Warhaft, Z., Turbulence suppression in a jet by means of a fine ring, *Phys. Fluids*, **6**, 1994, 328–333.

[24] Townsend, A. A., *The Structure of Turbulent Shear Flow (2nd edition)*, Cambridge University Press, Cambridge, 1976.

[25] Wygnanski, I., Champagne, F. and Marasli, B., On the large-scale structures in two-dimensional, small-deficit, turbulent wakes, *J. Fluid Mech.*, **168**, 1986, 31–71.

[26] Xu, G. and Antonia, R. A., Effect of different initial conditions on a turbulent round free jet, *Exp. Fluids*, **33**, 2002, 677–683.

[27] Xu, G. and Antonia, R. A., Effect of initial conditions on the temperature field of a turbulent round free jet, *Int. Comm. Heat Mass Transfer*, **29**, 2002, 1057–1068.

[28] Zaman, K. B. M. Q. and Hussain, A. K. M. F., Vortex pairing in a circular jet under controlled excitation. Part 1. General jet response, *J. Fluid Mech.*, **101**, 1980, 449–491.